On a High-Mirror Stellarator Reactor Exploratory Concept With Neutrons Concentrated on Centrifuge Liquids

V. Queral, I. Fernández, A. de Castro, D. Spong, S. Cabrera, V. Tribaldos, J. M. Reynolds, and E. Rincón

***Abstract*— In the framework of fusion energy research based on magnetic confinement, stellarators allow numerous degrees of freedom for the design of the magnetic trap and plasma shape. Taking advantage of these features, some plasma shapes might benefit several of the many integrated elements involved in commercial fusion reactors, like, e.g., decreasing the number, mass and complexity of replaced activated in-vessel components (IVC) (i.e., by using liquids), extraction of large power, tritium generation, and remote maintenance. Certainly, free-surface liquid materials were proposed for tokamaks and field-reversed configuration (FRC) to try to improve some of such elements, i.e., in advanced power extraction (APEX) studies. Some reactor-relevant quasi-isodynamic (QI) magnetic configurations exhibit a relatively straight sector of plasma and high magnetic mirror. The combination of those elements and possibilities in a single stellarator reactor concept might have some advantages, in spite of the uncertainties due to the current low technological readiness level (TRL). The proposed and studied reactor concept is based on a vacuum vessel having short curved sectors and longer wide cylindrical sectors, which encloses a high-mirror low-vertical-excursion magnetic configuration, and swirling liquids or rotating cylinders, which centrifuge molten Li salts located at the low field region. Thus, the molten salts (if possible covered by a thin layer of liquid lithium) would be located on the internal perimeter of the cylinder, to act as particle exhaust (except for helium), neutron power extractor, and tritium breeder. The high-mirror feature tries to concentrate the neutron power at the cylindrical sectors, which might avoid using breeding materials at the curved sectors. The different elements of the concept are exploratorily studied and defined, and the difficulties assessed.**

***Index Terms*— Centrifuge, fusion energy, high mirror, molten salt, stellarator.**

Manuscript received 2 October 2023; revised 13 December 2023; accepted 3 January 2024. This work was supported in part by the Agencia Estatal de Investigación (AEI), in part by the Ministry of Science and Innovation, and in part by the European Funds Fondo Europeo de Desarrollo Regional (FEDER) EU, under Grant PID2021-123616OB-I00, for the project "Study of improved stellarator assemblies consistent with proper in-vessel components for viable high-field stellarator reactors". The review of this article was arranged by Senior Editor R. Chapman. *(Corresponding author: V. Queral.)*

V. Queral, I. Fernández, A. de Castro, S. Cabrera, and E. Rincón are with the National Fusion Laboratory, Centro de Investigaciones Energéticas, Medioambientales y Tecnológicas (CIEMAT), 28040 Madrid, Spain (e-mail: vicentemanuel.queral@ciemat.es; ivan.fernandez@ciemat.es; Alfonso.DeCastro@ciemat.es; Santiago.Cabrera@ciemat.es; esther.rincon@ciemat.es).

D. Spong is with the Oak Ridge National Laboratory (ORNL), Oak Ridge, TN 37831 USA (e-mail: spongda@ornl.gov).

V. Tribaldos and J. M. Reynolds are with the Departamento de Física, Universidad Carlos III de Madrid, Leganés, 28911 Madrid, Spain (e-mail: vtribald@fis.uc3m.es; jreynold@fis.uc3m.es).

Color versions of one or more figures in this article are available at https://doi.org/10.1109/TPS.2024.3350985.

Digital Object Identifier 10.1109/TPS.2024.3350985

I. Introduction

EARLY integration of the many elements involved in the design of a commercial fusion energy plant is crucial in order to obtain a coherent and potentially lower cost plant. Some of the elements involved are: handling the power (heat) from neutrons and ionized particles impacting on the in-vessel components, tritium generation, plasma purity, remote replacement of activated components due to neutron damage or failure, facilities to remotely treat and temporary storage the activated metallic in-vessel components (IVC), the general structure of the reactor core and facilities, and a magnetic configuration appropriate for such needs. Stellarators allow numerous degrees of freedom for the design of the magnetic trap and plasma shape, which might facilitate the integration of some or most elements of a stellarator reactor.

Deuterium-tritium (DT) fueled magnetic fusion requires almost the full internal surface of the vacuum vessel covered by certain thickness (∼0.4–0.6 m) of a material containing lithium, usually called breeding material. This material is usually placed inside metallic structures located internally to the surface of the toroidal vacuum vessel, called blankets [1]. Also, the plasma-facing surface of the blankets [first wall (FW)] has to withstand a fraction of the energy coming from the plasma as ions, electrons, neutral particles, and Bremsstrahlung radiation. The main fraction of particles is directed to the divertor targets [2]. In some concepts, liquid materials, such as molten salts or lithium layers, were conceived to try to reduce solid blankets and/or divertor targets [3], [4], [5]. Thick or thin walls can be distinguished, which may be located at the FW, the divertors, or both locations [3]. These concepts would not only reduce or eliminate solid blankets (reducing their cost) but also importantly decrease the size and cost of the equipment and buildings [6] to remotely manipulate the replaced blankets and to temporarily store them (possibly cut and compacted) during some decades.

Nevertheless, the concepts having liquid walls thick enough to breed tritium need to advance and validate the methods to keep the breeding material in inverted positions, i.e., [3], feed and extract the flow into/from the vacuum vessel at high speed, avoid potential droplets and outgassing from the walls into the plasma, and to create fluid turbulence or high speeds at the divertorial areas (critical for low thermal conductivity molten salts if acting as divertor targets), among others. For fast-flowing thin molten metal layers on surfaces,

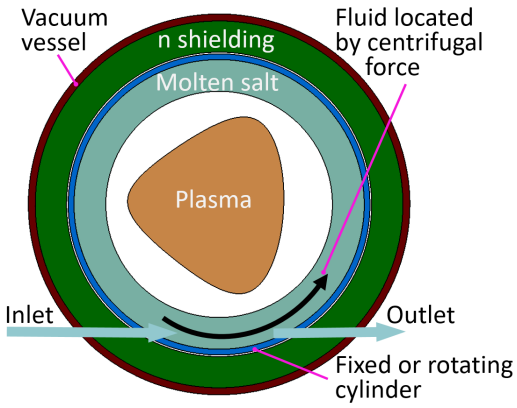

Fig. 1. Scheme of the elements of the concept.

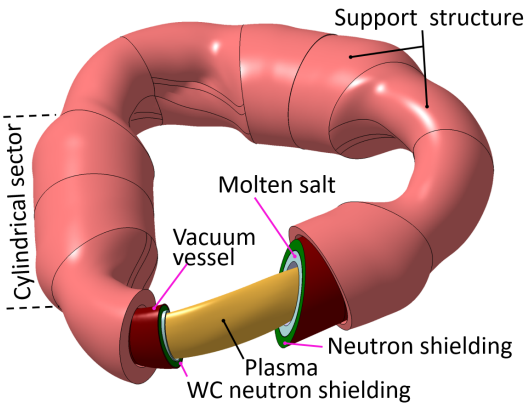

Fig. 2. Main elements of the reactor concept.

magnetohydrodynamic (MHD) issues are a concern and they are being studied and tested [7], [8]. Slow/medium flow concepts, which ameliorate the problems with MHD drag and surface stability of fast flow solutions, are treated in [9] and [10]. Indeed, the capillary porous system (CPS) offers capillary flow at the microscale while enhanced liquid stability [11].

In spite of the uncertainties due to the current low technological readiness level (TRL) of the concepts involved, a reactor concept (called ASTER-CP) that tries to integrate several advanced reactor elements is presented. The work tries to increase the knowledge on potential issues, find issues, and test some solutions. Divertorial elements (divertor magnetic means and targets) are not studied; coils, coil supporting structures, and fabrication methods were partially studied in previous works [12], [13], [14]; and only an outline of possible magnetic configurations is reported.

Section II describes the main elements of the reactor concept, Section III reports the contemplated molten salts and properties, the centrifuge concept and centrifuge liquid tests are reported in Section IV, an outline of the initial magnetic configurations is given in Section V, and the basic parameters and materials for the reactor concept are described in Section VI.

II. Elements of the Reactor Concept

The proposed stellarator reactor concept is based on a free-surface liquid material located inside cylinders by centrifugal force, which acts as breeder and FW (Fig. 1) and on a high-mirror quasi-isodynamic (QI) magnetic configuration to try to concentrate the neutron power mostly at the cylinders. A thin layer (thickness of millimeters or micrometers) of low-temperature lithium is intended to float on the molten salt for impurity pumping and reduction of hydrogen recycling, which resulted in enhanced plasma performance worldwide [10]. The shielding of Li-based molten salts significantly increases lifetime of the backwall structural material (a cylinder in this case) [3], so reducing activated components and activated masses. The high-mirror feature is intended for, as much as possible, concentration of neutrons at the cylinders, to try to avoid the use of liquid materials at the curved bean-shaped sectors of the stellarator (Fig. 2). Certainly, placing liquids in the bean-shaped sectors appears more difficult than in elliptical or egg-shaped sectors.

The main aim of the concept is to decrease the number, mass, and complexity of replaced activated in-vessel components, which are large, expensive to fabricate and activated, and to reduce the size and cost of the hot cells, which are necessary to manipulate and temporarily store the activated components. Nevertheless, a reduction in plasma performance is expected, due to the extra constraints on the plasma shape (see Section V). Still, uncertainties remain on some matters, e.g., potential influx of minuscule droplets or gases (radiolysis, transmutation) into the plasma from the molten salt and the feasibility of a thin layer of lithium on the molten salt (MHD, chemical compatibility and stability, and wetting).

III. Materials for the Liquid Layers

The materials and properties of the two layers, molten salt and floating lithium, are reported next.

A. Molten Salt

A relatively low melting point salt is required to allow low-temperature lithium on the molten salt. Enough retention of D and T isotopes and acceptable Li evaporation are mainly achieved for lithium up to 450 °C [10]. Several salts containing lithium have been compiled from the bibliography [15], [16]: FLiNaBe and FLiNaK (too low tritium breeding ratio (TBR) for this particular concept), LiF–PbF_2 (too high melting point, ~580 °C), FLiBe Li_2BeF_4 (slightly high melting point, 460 °C), LiCl–$BeCl_2$ (contains both the inconvenient Cl and Be), FLiBe LiF–BeF_2 ($LiBeF_3$), and LiCl–$PbCl_2$. The two last are candidate materials due to the difficulties of the other salts.

Their properties are as follows.

1) LiF–BeF_2 ($LiBeF_3$):

Properties at 500 °C (Some Properties Are for Li_2BeF_4):

Density ρ = 2055–2100 kg/m^3 [15].

Electric conductivity, σ (considered identical to Li_2BeF_4) = 155 S/m [17], and σ = 200 S/m [18]. Resistivity is ~6.5 × 10^{-3} Ω m, about 60 000 times higher than iron.

Thermal conductivity (of Li_2BeF_4) λ = 1 W/mK [19].

Specific heat C_p = 2400 J/(kg K) [19].

Dynamic viscosity ~0.022 Pa s ([20], extrapolated).

Melting point 380 °C [15].

Li_2BeF_4 appears relatively resistant to radiolysis [21], [22].

Eutectic Li_2BeF_4 gives TBR 1.2 for a free surface thickness of 0.55 m backed by ferritic steel [23]. TBR at the cylinders should be 1.2–1.3 to compensate the low or null tritium breeding at the curved sectors. For the current best magnetic configuration (Section V), still ~0.1 m thickness of breeding material is required at the curved sectors to obtain TBR ~1.05.

$LiBeF_3$ has relatively high viscosity (~0.022 Pa s), potential tendency to decompose into Li_2BeF_4 and BeF_2 [20], potential of BeF_2 to precipitate [20], the issues of using beryllium (toxic, scarce, and uranium impurities [24]), and it is highly corrosive.

2) LiCl–PbCl₂: Density (at 500 °C) $\rho = 4500$ kg/m^3 [15]. Melting point from 395 °C [16] to 420 °C [15] depending on composition. Other properties are still unknown to the authors.

LiCl–$PbCl_2$ avoids the use of Be but produces long-life activated ^{36}Cl; neutron shielding is poorer than for FLiBe [16] and appears to generate radiolytic $PbCl_4$ gas [15], [16]. The TBR for ^{37}Cl enriched option of the molten salt appears enough for the concept [16] (TBR = 1.17 for 90% enrichment, $LiCl_{40\%}PbCl_{2\text{-}60\%}$, cylindrical 1-D calculation, with FW and reactor-relevant breeding thickness).

B. Lithium Layer

In spite of the difficulties, molten lithium floating on the molten salt is pursued for: 1) pumping all the impurities in the plasma except for helium (this avoids large/difficult pumps under radiation environment and reduces the section/ports for pumping); 2) avoidance/reduction of potential gas influx from the molten salt to the plasma; and 3) promoting the favorable low recycling plasma regime.

Ideally, the Li layer should be as thick as possible (millimeters) due to thermal conductivity advantage. However, calculations/estimations on MHD and galinstan[1] tests (see Section IV-C) suggest important MHD drag.

IV. Liquids Kept by Centrifugal Force

Two methods are considered to locate the molten salts by centrifugal force: 1) swirling liquids on a fixed cylindrical wall, called "*swirling*" method and 2) rotating cylinders, somewhat similar to the method proposed by the company General Fusion for field-reversed configuration (FRC). This method may suffer from nuclear licensing issues and has not been deeply studied and tested yet. It is not further described in this work.

A. Justification of the Investigation of the Swirling Wall

In spite of possible showstoppers and low TRL of this concept, it is proposed to try to (similar reasons in [1] and [6]):

1) Lower the cost of replaced blankets. The estimated cost of EUROFER is in the range 50–100 €/kg [25], [26] (one case includes manufacturing cost). The real cost for ~5 t (t ≡ metric ton) production was 450 $/kg [27]. Considering a total of 10 000–15 000 t of EUROFER in replaced blankets for stellarators (left overs are not considered, which would increase the cost), deduced from [25], [28], and [29], this would imply a cost of 500–1500 M€ for only materials for all the replaced blankets. Also, the fabrication cost of only the FW (1000 m^2) for a full reactor and ten replacements may be deduced as 1500–3500 M€ from [30].
2) Lower the cost of the remote maintenance and storage facilities for the replaced activated elements. If common metallic-solid and geometrically complex IVCs are considered, the cost of such facilities appears relatively high, ~1000 M€ for the international thermonuclear experimental reactor (ITER) hot cell plus ~1600 M€ for related research and development [31]. Higher cost (perhaps one order of magnitude) is expected for a larger volume facility for a commercial reactor [6].
3) Importantly reduce the probability of leaks in the blankets, which may excessively lower the availability of the plant, as cited in [1]. Certainly, in fission plants, ~1% of all the U-pipes in fission steam generators in USA needed plugging to avoid leaks or future potential leaks due to corrosion, fretting, or other degradation [32].

[1]Trademarked.

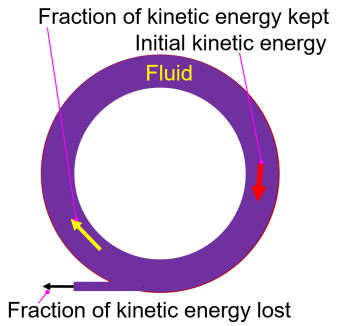

Fig. 3. Scheme of the outlet and kinetic energy separation.

B. Devised Swirling Concept for the Molten Salts. Test

Liquid free-surface methods for FWs and blankets are considered in the APEX studies, e.g., falling thin and thick walls, thin and thick walls kept by the combination of magnetic field and electrical currents, and swirling fluids [3].

Currently, swirling liquids are used in some fuel injectors for rocket engines to generate a proper spraying and mixing of the fuels. Also, a swirling concept was proposed for FRC magnetic configurations [3].

While the inlet flow appears simple, the outlet is more challenging, as already noted [3]. Indeed, the inlet flow speed is generated by the inlet pressure, but fast pumping at the outlet is complex (possible droplets) and inconvenient in a high-radiation environment. Thus, the next concept is concocted.

The fluid extraction would be produced at the external part of the fluid layer (higher minor radius) (Fig. 3), in order to: 1) more simply keep the uniformity of the liquid free surface; 2) keep a large part of the kinetic energy in the system in spite of the losses due to the outlet fluid; and 3) try to keep the thin lithium layer on the molten salt enough time in the system.

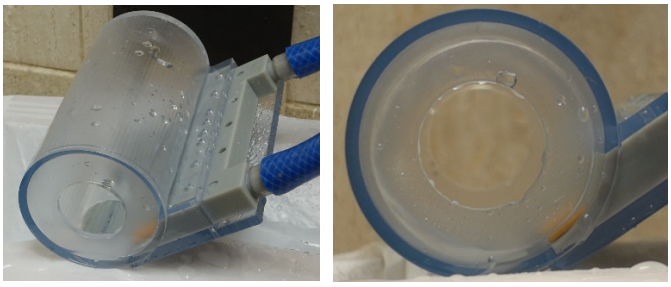

Fig. 4. Experimental 3-D-printed cylinder (left). Lateral view of the flow in permanent regime and fluid thickness (right).

A small-scale test was produced to initially validate the concept. The test is produced with pressurized water in a 3-D-printed transparent cylinder of 140 mm length and 70 mm diameter located in horizontal position (Fig. 4). The inlets and outlets can be changed in size and position up to some extent. After some planned experiments, a slit outlet at the middle of the cylinder length and inlets at the ends of the cylinder created a permanent regime of enough thickness, without droplets (Fig. 4) (see video recording in [33]).

The total flow rate (two inlets) was 0.2 dm^3/s, and the water speed at the tip of the inlet ∼4.5 m/s. The speed of the bulk fluid was ∼1.3 m/s at the middle of the cylinder (near the outlet) and ∼1.8 m/s near the inlets. The kinetic energy supplied by the two inlets was around 2 W.

The thickness of the fluid varied on the cylindrical surface. The minimum thickness was about 3–4 mm and the maximum 10–12 mm. As expected, the flow thickness at the intersection area of the two fluids (middle of the cylinder) was larger than at other areas. Improved thickness uniformity may be achieved by extra inlet nozzles or outlets.

Additionally, an experiment was produced at the minimum speed (lower speed gave rupture of the swirling), which resulted ∼0.8 m/s. This gives centrifugal acceleration 1.8 higher than gravity and a speed 35% higher than the theoretical minimum.

Computational fluid dynamics (CFD) simulations are being carried out to model the experimentally observed phenomena and to allow more reliable calculations for reactor size.

Slight inclination of the cylinder is favorable for QI magnetic configurations. Thus, two experiments were produced, at cylinder inclination of 10° and 16°. The experiment with 10° inclination resulted in no drops or other issue at the lower side of the cylinder. The experiment with 16° inclination resulted in drops and visible accumulation of liquid at the lower side of the cylinder.

C. Test of Galinstan in Rotating Cylinder Under B Field

In order to increase the knowledge on the matter and improve the analytical expressions for the MHD estimations, a simple experimental setup was prepared. A small slightly inclined insulating cylinder (plastic) of 12 mm internal diameter and 20 mm length was partially filled with Galinstan (eutectic alloy of gallium, indium, and tin) (Fig. 5). It rotates at adjustable speed. An N45 neodymium magnet 30 × 30 × 15 mm can be introduced/removed below the cylinder while rotating. A magnetic field from 0.4 to 0.1 T (depending on the position on the magnet surface and distance to Galinstan) is applied. The magnetic field is felt as temporarily variable by the rotating Galinstan, similar to the magnetic effect in the cylinders in the reactor design (Section VI-A).

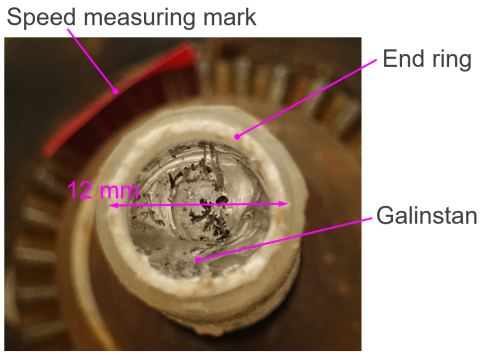

Fig. 5. Rotating cylinder for Galinstan experiment under magnetic field.

Using 0.6–0.7 mm thickness of Galinstan, at rotation speed ∼17 rps, the centrifuge flow was kept after introducing the magnet below the cylinder (small thickness fluctuations were observed). At ∼13 rps, the flow was shattered due to MHD drag. Initial calculations utilizing the MHD expressions cited in Section VI-A, and estimating the viscous drag from the Galinstan viscosity and certain speed gradient in the fluid layer gave approximately the same balance of viscosity/MHD as in the experiment.

An experiment having ∼1.2 mm thickness always stopped the centrifuge flow even up to 17 rps after the magnet introduction. In a reactor, the curvature radius and speeds are constrained, and the magnetic field is higher, creating difficulties for millimeter-thick Li layers (Section VI-B).

V. Magnetic Configuration

Only a summary of the methods and results is reported here. Enhanced methods and results will be produced and reported in a future work. Nevertheless, an initial magnetic configuration is necessary to advance the validation of the reactor concept, e.g., study the space for the molten salt, space for shielding, and initial nonoptimized size of the reactor. A three-period configuration has been selected since it is a low and reasonable number of periods, but a four or five periods configuration may be advantageous for coil simplicity or plasma performance. The magnetic configurations for ASTER-CP require high mirror-ratio, low vertical excursion, and reasonable neoclassical confinement and beta limit (β_{limit}).

The seed configuration for ASTER-CP was the UST_3 magnetic configuration utilized for the UST_3 stellarator [12]. This configuration came from a long optimization process for a low aspect ratio and high beta QI configuration. QIP3 [34], quasi-poloidal stellarator (QPS) of three periods [35], and the configurations in [36] were the origin for such optimization process. The aspect ratio and vertical excursion of the UST_3 configuration were changed, so as the last closed flux surface (LCFS) were able to fit inside cylinders, resulting the initial LCFS (see Fig. 6).

A series of modified configurations, LCFS_m (m is the order number in a total of n configurations calculated, $m = 1, \ldots, n$) are generated by a code called calculator of stellarators

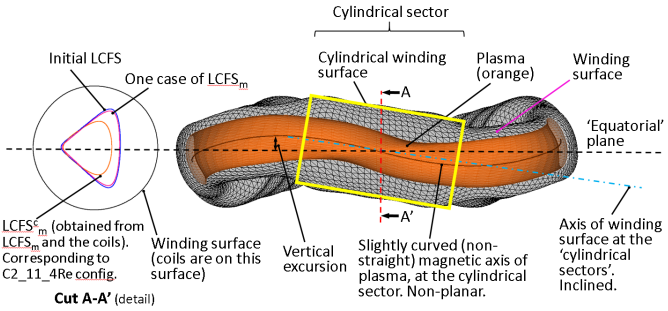

Fig. 6. Scheme of the involved elements and concepts.

(CASTELL) [37], by varying the mirror ratio (MR) and the vertical excursion (Fig. 6) of the initial LCFS. Additionally, the distance from the cylindrical winding surface to the LCFS and the length of the cylinder are varied.

CASTELL contains a suite of Information Technology (IT) methods and codes and calls and connects them. The suite includes, among others, a guiding center orbits generator, geometrical treatment of toroidal surfaces, and approximate neoclassical confinement calculator. Also, it can automatically call the codes NESCOIL [38], variational moments equilibrium code (VMEC) [39], and code for ballooning rapid analysis (COBRA) [40]. CASTELL was used time ago to obtain magnetic configurations for UST_1, UST_2, and UST_3 stellarators [12], [37].

Departing from each LCFS$_m$, CASTELL obtains the current potential on the winding surface (calling NESCOIL). From this potential, a set of modular coils are obtained and their magnetic field (obtained by Biot Savart from the coil geometry) is integrated to follow particles. From the magnetic field lines distribution, a more realistic LCFS is obtained, named LCFS^c_m. Notice that the LCFS^c_m surface can differ significantly from the objective surface (LCFS$_m$) as can be seen in Fig. 6, left. For LCFS^c_m, approximate neoclassical confinement was estimated by CASTELL and beta limit by VMEC [39] and COBRA [40].

The explained procedure is repeated for each configuration m.

From all the LCFS^c_m configurations studied, two cases stand out.

1) *Configuration C7_12_5_9C:* It exhibits high MR = 3.8, $\beta_{\text{limit}} \sim 1.5\%$, and acceptable distance from the cylinder to the plasma. The neoclassical confinement of this configuration was recalculated by MOCA code [41]. The confinement at the low collisionality regime resulted ~10 times lower than that of the QIP3 configuration.
2) *Configuration C2_11_4Re:* It has MR = 3, $\beta_{\text{limit}} \sim 2\%$, and also acceptable distance from the cylinder.

In Fig. 2, the space for the molten salt (0.55 m) and the WC shielding at the inboard high-field curved section (0.4 m) are allocated for the C2_11_4Re configuration.

A. Remarks on the Results

The notable deviation of LCFS^c_m from LCFS$_m$ appears to be caused by the relatively large distance from the winding surface to the LCFS$_m$ at certain areas of the "cylindrical sector." This implies that the plasma properties of the LCFS^c_m configuration differ from the ones for LCFS$_m$, usually for the worse. Nevertheless, since many LCFS$_m$ were computed, some of them still might retain reasonable properties, as may be the case of C7_12_5_9C and C2_11_4Re configurations.

The obtained values of β_{limit} and confinement are low and likely unsatisfactory for a reactor. It represents one of the difficulties of the concept found during the investigation. $\beta_{\text{limit}} \sim 3\%$ (about twice of C7_12_5_9C and C2_11_4Re configurations), and confinement reduction of factor 5 may be considered satisfactory if substantial economic advantages are obtained in exchange. Certainly, the difference in confinement from W7-X and large helical device (LHD)-inward configurations is about factor 5 [42], and still, LHD-like force free helical reactor (FFHR) reactors may be considered. β_{limit} higher than 3% would be convenient to produce higher power at the same or lower magnetic field. However, enough power (4 GW_{th}) was obtained at slightly high magnetic field (higher cost, $B_0 = 8.2$ T, see the next section).

Further optimization will be produced in the future to try to increase confinement and β_{limit} at least twice, while still fitting in cylinders.

VI. Basic Parameters and Materials for the Reactor Concept

The average major radius of the C2_11_4Re and C7_12_5_9Ca configurations is $R = 14.5$ m for a plasma volume of 500 m^3. The average is taken until the definitive magnetic configuration is decided. It results in an aspect ratio $A = 11$. Following the same expressions and methods for the ignition-capable experimental fusion reactor i-ASTER [43], and assuming that $\beta = 3\%$ is achievable, the average magnetic field at the magnetic axis is $B_0 = 8.2$ T and the produced fusion power ~4 GW_{th}. The plasma is considered to be under ignition condition. Shielding and breeding materials fit in the available space (Fig. 2).

Considering C2_11_4Re (Fig. 2), the internal diameter of the cylinder is $D_{\text{cyl}} = 5$ m, length of the cylinder $L_{\text{cyl}} = 12$ m, thickness of the molten salt 0.55 m, fluid volume in one cylinder ~90 m^3, and mass ~200 t (FLiBe) and ~400 t (LiCl–$PbCl_2$).

The average speed of the bulk flow is taken as 8 m/s, which gives a reasonable safety factor of 3 ($a_{\text{centrifuge}} \sim= 30$ m/s^2). The total kinetic energy of the fluid per cylinder is ~7 MJ.

FLiBe LiF–BeF_2 is the reference molten salt for ASTER-CP and the salt $LiCl_{40\%}$-$PbCl_{2\text{-}60\%}$ a back-up option (Section III).

The material for the cylinder, which acts as a backwall, has not been decided yet. Metals might be possible if relatively large kinetic power can be injected into the system to avoid the considerable MHD drag. Fiber-reinforced ceramics SiC, ZrO_2, and Al_2O_3 are being studied in case they were required.

A. Power Losses in the Molten Salt

Despite the low conductivity of FLiBe (~200 S/m, four orders of magnitude lower than for Li), an estimation of MHD is needed to discover possible issues.

The hydraulic friction losses (no MHD) are estimated ~0.8 MW for FLiBe at 500 °C (Darcy friction factor of 0.013).

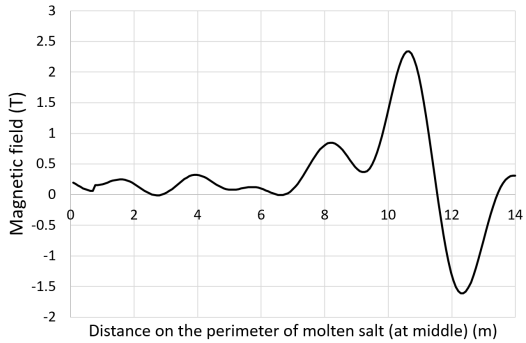

Fig. 7. Variation of the normal magnetic field on a poloidal cut at the end of the cylinder.

The energy losses due to MHD effect, for FLiBe at 500 °C, are estimated following the general expression n.7 in [44], considering a ceramic cylinder with conductivity $\sigma < 1$ S/m (the three ceramics cited fulfill this condition), assimilating the free flow to a rectangular conduit (it appears a conservative assumption) and considering kinetic energy supplied throughout the full liquid volume.

The normal (normal to the cylinder surface, on a poloidal cut) magnetic field B_n on the surface of the cylinder ends is shown in Fig. 7. B_n is more uniform and lower at the middle of the cylinder.

The observed field variation (Fig. 7) corresponds to the case of a varying magnetic field with $z1/z2 = 10/12$ ([45, Fig. 10], $z2 - z1$ is the normalized length of the magnetic field slope), which would result in a power loss of ∼0.1 MW. If a slow variation of the field is considered, according to [46], the total pressure drop can be approximated by the integral of the pressure drop from each (differential) section. In this manner, the pressure drop due to the variable magnetic field results <∼1000 Pa and the power losses ∼0.1 MW. This is coherent with the fact that, for insulating walls, the pressure drop due to the varying magnetic field for any $z1/z2$ results of the order or lower than the effect of a constant magnetic field in a similar normalized pipe length [47]. The pressure losses due to the fast expansion of the flow at each inlet nozzle, estimated by Lielausis expressions [48], for the two nozzles (17 m/s tip-inlet speed), result ∼0.1 MW. Summing-up the three values (conservatively considered from [45]) results 0.3 MW of power losses due to MHD.

Adding the hydrodynamic and MHD losses and considering a safety factor of 1.5 results in 1.65 MW per cylinder. This can be compensated by the power (1.7 MW) from the two inlets at a flow speed of 17 m/s and 30% larger section (scaled) than in the experiment in Section IV-B.

Thus, the MHD on the molten salt is not currently considered a showstopper for the concept. Further calculations and CFD simulations are being produced to increase the accuracy of the estimations and to discover other potential MHD effects that might hinder the feasibility of the concept.

B. Issue With the Thickness of Li on the Molten Salt

Applying the same expressions and methods as in Section VI-A (see also Section IV-C), without considering the effect of surface tension, for Li on molten salt of conductivity $\sigma < 220$ S/m and thickness 0.55 m (here, the molten salt acts as the wall of a pipe), the maximum thickness of Li layer is estimated. It results in ∼10 μm thickness for field as in Fig. 7 and ∼30 μm for half such field. The thickness obtained is rather thin; thus, surface tension might allow thicker layers. Consequently, the possibility of centrifuging a thick (∼1–3 mm) Li layer on the molten salt is dubious and needs further studies and innovation.

C. Potential Issues and Uncertainties of the Reactor Concept

Potential minuscule droplets or spray influx into the plasma from the walls, potential influx of gases from the molten salts due to radiolysis or transmutation (outgassing should be avoided by proper vacuum degassing), chemical compatibility and interaction (i.e. degree of wetting, dissolution) of a layer of lithium on the molten salt, maximum thickness of lithium due to MHD limits, potential excessive erosion–corrosion of the surface of the cylinder (refurbishment of the eroded surface may be conceived), potential difficulties for enough increase of the neoclassical confinement and β_{limit}, the method to keep ∼0.1 m thickness of breeding material at the curved sectors (or increase the MR to avoid it), the in-vessel interface of the cylinder with the curved sector, and FW type for the curved sectors (perhaps a CPS) are current uncertainties or issues of the concept. The corrosion of the metallic or ceramic cylinder and loop systems, by FLiBe or other molten salt, is of particular relevance. Corrosion severity will be critically influenced by the salt chemistry, the temperature in the cylinder and in the loop system, the flow velocity, existence of certain dissolved impurities [i.e., F, tritium fluoride (TF)], redox condition of the salt, and the quality of continuous monitoring and purification of the salt.

VII. Conclusion

A reactor concept based on centrifuge molten salts in cylinders and high concentration of neutrons at the cylinders has been outlined. Initial calculations/estimations have discovered certain issues and limits of the concept, like the thickness of the lithium layer, but strong showstoppers have not been found yet. CFD fluid calculations are being produced. Experiments of rotating Galinstan under higher field and experiments of interaction of lithium floating on molten salt are being prepared.

Acknowledgment

The authors are grateful to the CIEMAT researchers: Daniel Alegre for discussions on plasma-wall-Li, Alejandro Moroño (materials under radiation), Edilberto Sánchez (parallel computing), Fernando R. Urgorri (liquids MHD), María Gonzalez (ceramics), Francisco Tabarés; Arnold Lumsdaine (ORNL, USA), Egemen Kolemen (liquids MHD; PPPL, USA), Raúl Sánchez (U. CIII Madrid, COBRA assistance), and IPP Max-Planck M.I. Mikhailov, J. Nührenberg et al. [34] for supplying the QIP3 magnetic configuration. Funding for APC: Universidad Carlos III de Madrid (Agreement CRUE-Madroño 2024).

References

[1] M. Abdou et al., "Blanket/first wall challenges and required R&D on the pathway to DEMO," *Fusion Eng. Design*, vol. 100, pp. 2–43, Nov. 2015.

[2] P. C. Stangeby and G. M. McCracken, "Plasma boundary phenomena in tokamaks," *Nucl. Fusion*, vol. 30, no. 7, pp. 1225–1379, Jul. 1990.

[3] M. A. Abdou et al., "On the exploration of innovative concepts for fusion chamber technology," *Fusion Eng. Design*, vol. 54, no. 2, pp. 181–247, Feb. 2001.

[4] R. E. Nygren and F. L. Tabarés, "Liquid surfaces for fusion plasma facing components—A critical review. Part I: Physics and PSI," *Nucl. Mater. Energy*, vol. 9, pp. 6–21, Dec. 2016.

[5] F. L. Tabarés, E. Oyarzabal, A. B. Martin-Rojo, D. Tafalla, A. de Castro, and A. Soleto, "Reactor plasma facing component designs based on liquid metal concepts supported in porous systems," *Nucl. Fusion*, vol. 57, no. 1, Jan. 2017, Art. no. 016029.

[6] T. G. Brown, "Three confinement systems—Spherical tokamak, standard tokamak, and stellarator: A comparison of key component cost elements," *IEEE Trans. Plasma Sci.*, vol. 46, no. 6, pp. 2216–2230, Jun. 2018.

[7] F. Saenz, Z. Sun, A. E. Fisher, B. Wynne, and E. Kolemen, "Divertorlets concept for low-recycling fusion reactor divertor: Experimental, analytical and numerical verification," *Nucl. Fusion*, vol. 62, no. 8, Aug. 2022, Art. no. 086008.

[8] E. Kolemen, M. Hvasta, R. Majeski, R. Maingi, A. Brooks, and T. Kozub, "Design of the Flowing LIquid Torus (FLIT)," *Nucl. Mater. Energy*, vol. 19, pp. 524–530, May 2019.

[9] D. N. Ruzic, W. Xu, D. Andruczyk, and M. A. Jaworski, "Lithium–metal infused trenches (LiMIT) for heat removal in fusion devices," *Nucl. Fusion*, vol. 51, no. 10, Oct. 2011, Art. no. 102002.

[10] A. de Castro, C. Moynihan, S. Stemmley, M. Szott, and D. N. Ruzic, "Lithium, a path to make fusion energy affordable," *Phys. Plasmas*, vol. 28, no. 5, May 2021, Art. no. 050901.

[11] A. V. Vertkov, I. E. Lyublinski, F. Tabares, and E. Ascasibar, "Status and prospect of the development of liquid lithium limiters for stellarotor TJ-II," *Fusion Eng. Design*, vol. 87, no. 10, pp. 1755–1759, Oct. 2012.

[12] V. Queral, E. Rincón, A. Lumsdaine, S. Cabrera, and D. Spong, "Composites and additive manufacturing for high-field coil supports for stellarators," *Fusion Eng. Design*, vol. 169, Aug. 2021, Art. no. 112477.

[13] V. Queral, E. Rincón, S. Cabrera, and A. Lumsdaine, "Evaluation of metal additive manufacturing for high-field modular-stellarator radial plates and conductors," *Nucl. Mater. Energy*, vol. 30, Mar. 2022, Art. no. 101149.

[14] V. Queral, S. Cabrera, E. Rincón, E. Barbarias, F. Santos, and J. M. Gutiérrez, "Embedded conductors in solidified molten metal for winding packs for high-field stellarators," *Fusion Eng. Design*, vol. 190, May 2023, Art. no. 113495.

[15] R. Boullon, J.-C. Jaboulay, and J. Aubert, "Molten salt breeding blanket: Investigations and proposals of pre-conceptual design options for testing in DEMO," *Fusion Eng. Design*, vol. 171, Oct. 2021, Art. no. 112707.

[16] T. D. Bohm and B. A. Lindley, "Initial neutronics investigation of a chlorine salt-based breeder blanket," *Fusion Sci. Technol.*, vol. 79, no. 8, pp. 995–1007, Nov. 2023.

[17] J. Takeuchi, S.-I. Satake, N. B. Morley, T. Kunugi, T. Yokomine, and M. A. Abdou, "Experimental study of MHD effects on turbulent flow of flibe simulant fluid in circular pipe," *Fusion Eng. Design*, vol. 83, nos. 7–9, pp. 1082–1086, Dec. 2008.

[18] W. R. Grimes and S. Cantor, "Molten salts as blanket fluids in controlled fusion reactors," Oak Ridge Nat. Lab., Oak Ridge, Tennessee, Tech. Rep. ORNL-TM-4047, Dec. 1972.

[19] M. S. Sohal, M. A. Ebner, P. Sabharwall, and P. Sharpe, "Engineering database of liquid salt thermophysical and thermochemical properties," Idaho National Lab., Idaho Falls, ID, USA, Tech. Rep. INL/EXT-10-18297, Mar. 2010.

[20] F. Carotti et al., "Experimental and modeling studies of over-cooling transients in fluoride-salt cooled high-temperature reactors," in *Proc. 16th NURETH*, Chicago, IL, USA, Aug./Sep. 2015.

[21] L. Davis et al., "Radiolytic production of fluorine gas from MSR relevant fluoride salts," *Nucl. Sci. Eng.*, vol. 197, no. 4, pp. 633–646, Apr. 2023.

[22] C. Forsberg, L.-W. Hu, P. Peterson, and K. Sridharan, "Fluoride-salt-cooled high-temperature reactor (FHR) for power and process heat," MIT, Cambridge, MA, USA, Tech. Rep. MIT-ANP-TR-157, Dec. 2014.

[23] M. Z. Youssef and M. A. Abdou, "Heat deposition, damage, and tritium breeding characteristics in thick liquid wall blanket concepts," *Fusion Eng. Design*, vols. 49–50, pp. 719–725, Nov. 2000.

[24] B. N. Kolbasov, V. I. Khripunov, and A. Y. Biryukov, "On use of beryllium in fusion reactors: Resources, impurities and necessity of detritiation after irradiation," *Fusion Eng. Des.*, vols. 109–111, pp. 480–484, 2016.

[25] J. F. Lyon et al., "Systems studies and optimization of the ARIES-CS power plant," *Fusion Sci. Technol.*, vol. 54, no. 3, pp. 694–724, Oct. 2008.

[26] T. J. Dolan, K. Yamazaki, and A. Sagara, "Helical fusion power plant economics studies," *Fusion Sci. Technol.*, vol. 47, no. 1, pp. 60–72, Jan. 2005.

[27] A. Ying, "HCCB TBM design and fabrication plan and cost estimate," ITER-TBM UCLA, Univ. California—Los Angeles, Los Angeles, CA, USA, Presentation, Dec. 2005.

[28] T. Amano, C. D. Beidler, E. Harmeyer, F. Herrnegger, and A. Kend, "Progress in Helias reactor studies," in *Proc. 12th Int. Stellarator Workshop*, Madison, WI, USA, Sep./Oct. 1999, pp. 1–23.

[29] A. Sagara et al., "Improved structure and long-life blanket concepts for Heliotron reactors," *Nucl. Fusion*, vol. 45, no. 4, pp. 258–263, Apr. 2005.

[30] H. Neuberger et al., "Evaluation of conservative and innovative manufacturing routes for gas cooled test blanket module and breeding blanket first walls," *Fusion Eng. Design*, vol. 146, pp. 2140–2143, Sep. 2019.

[31] *Brochure 'Robotics for a Safer World, Robotics and Artificial Intelligence in Extreme Environments*, U.K. Res. Innov., Swindon, U.K., 2018.

[32] *Electric Power Monthly*, document DOE/EIA-0226(95/08), Energy Inf. Admin., Washington, DC, USA, Aug. 1995.

[33] *VideoRecording*. Accessed: Aug. 2023. [Online]. Available: https://www.youtube.com/watch?v=bMJVOkHZ9Sc

[34] M. J. Mikhailov et al., "Comparison of the properties of QI configurations for different number of periods," in *Proc. 31st EPS Conf. Plasma Phys.*, London, U.K., Jun. 2004, pp. 1–4.

[35] S. P. Hirshman et al., "High-beta QPS stellarator configurations," in *Proc. 29th EPS Conf. Plasma Phys. Contr. Fusion*, vol. 26, Montreux, Switzerland, Jun. 2002, pp. 17–21.

[36] V. Queral, "Generic configuration stellarator based on several concentric Fourier windings," 2016, *arXiv:1601.02908*.

[37] V. Queral, "Rapid manufacturing methods for geometrically complex nuclear fusion devices: The UST_2 stellarator," Ph.D. thesis, Departamento de Física, Universidad Carlos III de Madrid, Getafe, Spain, 2015.

[38] P. Merkel, "Solution of stellarator boundary value problems with external currents," *Nucl. Fusion*, vol. 27, no. 5, p. 867, 1987.

[39] S. P. Hirshman and J. C. Whitson, "Steepest-descent moment method for three-dimensional magnetohydrodynamic equilibria," *Phys. Fluids*, vol. 26, no. 12, pp. 3553–3568, 1983.

[40] R. Sanchez, S. P. Hirshman, J. C. Whitson, and A. S. Ware, "COBRA: An optimized code for fast analysis of ideal ballooning stability of three-dimensional magnetic equilibria," *J. Comput. Phys.*, vol. 161, no. 2, pp. 576–588, Jul. 2000.

[41] V. Tribaldos, "Monte Carlo estimation of neoclassical transport for the TJ-II stellarator," *Phys. Plasmas*, vol. 8, no. 4, pp. 1229–1239, Apr. 2001.

[42] C. D. Beidler et al., "Demonstration of reduced neoclassical energy transport in Wendelstein 7-X," *Nature*, vol. 596, pp. 221–226, Aug. 2021.

[43] V. Queral, F. A. Volpe, D. Spong, S. Cabrera, and F. Tabarés, "Initial exploration of high-field pulsed stellarator approach to ignition experiments," *J. Fusion Energy*, vol. 37, no. 6, pp. 275–290, Dec. 2018.

[44] I. Michael, "Study of MHD problems in liquid metal blankets of fusion reactors," Institut füer Reaktorbauelemente, Kernforschungszentrum, Karlsruhe, Germany, Tech. Rep. KFK 3839, Dec. 1984.

[45] H. Kumamaru, "MHD flows through circular pipe in magnetic field inlet region and outlet region," *Fusion Sci. Tech.*, vol. 79, no. 2, pp. 135–150, 2023.

[46] K. Miyazaki, K. Konishi, and S. Inoue, "MHD pressure drop of liquid metal flow in circular duct under variable transverse magnetic field," *J. Nucl. Sci. Technol.*, vol. 28, no. 2, pp. 159–161, Feb. 1991.

[47] H. Kumamaru, K. Shimoda, and K. Itoh, "Three-dimensional numerical calculations on liquid-metal MHD flow through circular pipe in magnetic-field inlet-region," *J. Nuclear Sci. Tech.*, vol. 44, no. 5, pp. 714–722, 2007.

[48] O. Lielausis, "Liquid-metal magnetohydrodynamics," *Atomic Energy Rev.*, vol. 13, no. 3, pp. 527–581, 1975.